



Binding of red form of Orange Carotenoid Protein (OCP) to phycobilisome is not sufficient for quenching

Wenjing Lou^{a,1}, Dariusz M. Niedzwiedzki^{b,c,1}, Ruidong J. Jiang^d, Robert E. Blankenship^{a,d}, Haijun Liu^{a,d,*}

^a Department of Biology, Washington University in St. Louis, St. Louis, MO 63130, USA

^b Center for Solar Energy and Energy Storage, Washington University in St. Louis, St. Louis, MO 63130, USA

^c Department of Energy, Environmental & Chemical Engineering, Washington University in St. Louis, St. Louis, MO 63130, USA

^d Department of Chemistry, Washington University in St. Louis, St. Louis, MO 63130, USA

ARTICLE INFO

Keywords:

Orange Carotenoid Protein
Excitation energy quenching
Site-directed mutagenesis
OCP–phycobilisome quenching complex

ABSTRACT

The Orange Carotenoid Protein (OCP) is responsible for photoprotection in many cyanobacteria. Absorption of blue light drives the conversion of the orange, inactive form (OCP^O) to the red, active form (OCP^R). Concomitantly, the N-terminal domain (NTD) and the C-terminal domain (CTD) of OCP separate, which ultimately leads to the formation of a quenched OCP^R–PBS complex. The details of the photoactivation of OCP have been intensely researched. Binding site(s) of OCP^R on the PBS core have also been proposed. However, the post-binding events of the OCP^R–PBS complex remain unclear. Here, we demonstrate that PBS-bound OCP^R is not sufficient as a PBS excitation energy quencher. Using site-directed mutagenesis, we generated a suite of single point mutations at OCP Leucine 51 (L51) of *Synechocystis* 6803. Steady-state and time-resolved fluorescence analyses demonstrated that all mutant proteins are unable to quench the PBS fluorescence, owing to either failed OCP binding to PBS, or, if bound, an OCP–PBS quenching state failed to form. The SDS-PAGE and Western blot analysis support that the L51A (Alanine) mutant binds to the PBS and therefore belongs to the second category. We hypothesize that upon binding to PBS, OCP^R likely reorganizes and adopts a new conformational state (OCP^{3rd}) different than either OCP^O or OCP^R to allow energy quenching, depending on the cross-talk between OCP^R and its PBS core-binding counterpart.

1. Introduction

All oxygenic photosynthetic organisms have developed a protective mechanism known as non-photochemical quenching (NPQ) to dissipate excess light energy as heat at the level of the photosynthetic antenna [3–7]. In cyanobacteria and red algae, the phycobilisome (PBS) is the primary light-harvesting antenna complex. It harvests solar radiation and transfers the excitation energy to the reaction centers of either photosystem I (PSI) or photosystem II (PSII) or both [8–10]. In many cyanobacteria, NPQ is triggered and actuated by a soluble protein, Orange Carotenoid Protein (OCP), hosting a single molecule of carotenoid, 3-hydroxyechinenone (3'-hECN) [4,11]. Exposure to blue-green light affects OCP in a way that it converts to an active, red form OCP^R. The OCP^R binds to the PBS and quenches excited phycocyanobilins resulting in reduced excitation energy arriving at both reaction centers, thus protecting the photosystems from over-excitation and

subsequent photodamage [11]. This process is known as OCP-mediated NPQ.

OCP, unique to cyanobacteria, was first isolated and reported by Krogmann's group in 1981 [12]. It was then crystallized and its structure was determined in 2003 by Kerfeld et al., [13]. OCP consists of two structural domains (or modules), the α -helical N-terminal domain (NTD) and the mixed α/β C-terminal domain (CTD), which are joined by a flexible linker domain, with carotenoid 3'-hECN non-covalently bound in the inter-domain cavity formed by both NTD and CTD [11,13,14]. OCP can interconvert between two forms: the inactive, orange form (OCP^O) and the active, red form (OCP^R). In darkness, OCP is “dormant” in its inactive OCP^O form with a characteristic 3'-hECN absorption spectrum peaking at 475 nm and 495 nm [15,16]. In this OCP state, the carotenoid pigment interacts with both NTD and CTD through multiple weak molecular forces such as hydrogen bonds (H-bonds), hydrophobic interactions, and van der Waals contacts [13].

* Corresponding author at: Department of Chemistry, Washington University in St. Louis, St. Louis, MO, USA.

E-mail address: liuhaijun@wustl.edu (H. Liu).

¹ Contributed equally to this work.

Intense white or blue light drives 3'-hECN to adopt a completely different conformation that breaks the interactions with the CTD, resulting in a complete separation of NTD and CTD [17–19]. The carotenoid pigment becomes more planar and moves 12 Å deeper into the NTD, and is almost totally encased in NTD with only the β-keto-rings exposed [20]. OCP^R is metastable and spontaneously reverts back to OCP^O in darkness [17,21]. It is believed that OCP^R is the only form to interact with the PBS and induce quenching of PBS fluorescence. OCP^R seems to only bind to a PBS with a core structure containing allophycocyanin and execute NPQ there [22–26]. It was demonstrated that the CTD acts as the regulator domain, conferring the photo-conversion of OCP and regulating the activity of OCP by interacting with the fluorescence recovery protein (FRP) [27]. The NTD is the effective quencher domain [28]. In the absence of the CTD, the carotenoid-binding NTD is known as the red carotenoid protein (RCP). It constitutively binds to a PBS and quenches its fluorescence comparably to the OCP^R [27,29]. The crystal structure of the RCP was reported by Kerfeld's group in 2015 and shows not much conformational differences compared to the NTD of OCP^O [20]. The accurate structural binding site and OCP^R binding stoichiometry to the PBS core are still controversial owing to the absence of a cyanobacterial PBS structure and OCP-PBS complex structure at atomic resolution [24,30–33].

The exact molecular mechanism of OCP-PBS quenching is still unknown [6,33–36]. The consensus is that there are two states of OCP: i.e., OCP^O and OCP^R with some transient intermediates between two states [37–39]. Both OCP^O and OCP^R are energetically suitable for efficient quenching of PBS [16,40], albeit the detailed mechanism remains elusive. So, it is indeed the protein conformation that OCP^R adopts that qualifies it for competent association with the PBS core. It is generally accepted that once OCP^R is formed, it is sufficient to quench the fluorescence of a PBS [6,22]. In order to execute PBS excitation energy quenching, OCP^R has to first bind to the PBS core, forming an OCP^R-PBS binding complex. Now the question arises: is simple association of OCP^R to PBS enough to trigger OCP-mediated NPQ?

In this report, a series of OCP mutants at Leucine 51 (L51), an amino acid (AA) residue located in a loop region in OCP and located in the interface between NTD and CTD, were constructed and their quenching capabilities were recorded using steady-state and time-resolved fluorescence. One of those OCP mutants, L51A OCP, evidently converts to red form and binds to the PBS but is not able to quench PBS fluorescence and demonstrates that the OCP-PBS binding/quenching mechanism may be more complex than expected.

2. Materials and methods

2.1. Plasmid construction

The DNA fragment containing *crtB*, *crtE*, *crtI*, and *crtY* was amplified from the plasmid K274200 (gift from iGEM, parts.igem.org/Part:BBa_K274200) using primers carotenoid-1/2 (Table S1). The fragment was cloned into the *PstI/EcoRI* site of pACYCDuet™-1 plasmid (Novagen, Madison, WI, USA) under the control of the constitutive promoter of R0011 (iGEM). The resulting plasmid was named as pACY-caro, containing a chloramphenicol resistance fragment. pBAD-CrtO (a gift from Dr. D. Kirilovsky [41]), which contains *slr0088* gene from *Synechocystis* PCC 6803 (thus *Synechocystis* 6803) under the control of an arabinose inducible promoter (*araBAD*), and an ampicillin resistance marker, was used as reported [41]. The *slr1963* DNA fragment was amplified from the genome of *Synechocystis* 6803 using primers *slr1963-1/2* (Table S1), and then was introduced into the *PstI* site of pCDFDuet-1™ (Novagen, Madison, WI, USA) under the control of T7-lac promoter to create the pDuet-OCP plasmid. The single point mutations L51A, L51D, L51K, L51T, and T52A were introduced by site-directed mutagenesis, using the pDuet-OCP plasmid as a template and primers are listed in Table S1.

2.2. OCP expression and isolation

The pDuet-OCP, pBAD-CrtO and pACY-caro were simultaneously transformed into DE3 competent cells (BL21-gold, F⁻ ompT hsdS(r_B⁻ m_B⁻) dcm⁺ Tet^r gal λ(DE3) endA Hte, Agilent Technologies, Santa Clara, CA, USA). The holo-OCP was induced as described by de Carbon et al. with minor modifications [41]. The transformed cells were grown overnight in Terrific Broth (TB) medium, containing 50 mg ml⁻¹ ampicillin, 50 mg ml⁻¹ streptomycin, and 25 mg ml⁻¹ chloramphenicol at 37 °C. The overnight culture was diluted using fresh TB medium and was grown at 37 °C for about 6 h until OD₆₀₀ = 0.6. Arabinose was then added (to a final concentration of 0.02%) to induce the expression of CrtO. The culture was grown overnight at 37 °C. Then, the culture was diluted 10 times using fresh TB medium, containing 0.02% arabinose and antibiotics and was grown at 37 °C until OD₆₀₀ = 1.0. The expression of OCP was induced by adding 0.2 mM isopropyl-β-D-thiogalactoside (IPTG) and the cells were grown overnight at 28 °C. The cells were harvested and stored at -80 °C.

The harvested cells were broken by passing twice through a French press. The holo-OCP was isolated and purified using HisTrap HP affinity chromatography followed by HiTrap Q HP ion exchange chromatography (Sigma, St. Louis, MO, USA), as described previously [17,30].

2.3. Isolation of the wild type (WT)-PBS, CB-PBS and OCP-PBS

The wild type (WT-) and CB-PBS were isolated from the WT and the CB mutant of *Synechocystis* sp. PCC 6803, respectively, according to the methods described previously [22,42,43] with minor modifications. Wild type and the CB mutant that lacks the intermediary and the core-distal phycocyanin hexamer and only contains core-proximal phycocyanin hexamer were grown in BG11 at continuous fluorescent illumination conditions (30 μmol photons m⁻²s⁻¹), bubbled with air. Cells were harvested, resuspended in 0.8 M pH 7.5 potassium phosphate buffer (KP) and then broken by passing through a French press (twice, 20,000 psi) in the presence of protease inhibitor cocktail (Thermo Fisher Scientific, Waltham, MA, USA). The broken cells were incubated with 1% Triton X-100 at room temperature for 30 min with gentle shaking. The cell debris was removed by centrifugation at 20,000 rpm using a SS-34 rotor (Sorvall Evolution RC, Thermo Scientific, Waltham, MA, USA) at 23 °C for 30 min. The supernatant was immediately loaded onto a sucrose gradient, containing layers of 2.0 M, 1.0 M, 0.75 M, 0.5 M, 0.25 M sucrose solutions in 0.8 M KP buffer (pH 7.5) in a SW 32 Ti centrifuge tube (Beckman Coulter, Indianapolis, IN, USA). The sucrose gradient was spun at 32,000 rpm using a SW 32 Ti rotor at 23 °C overnight. The blue band between 1.0 M and 2.0 M sucrose layers was collected and the absorption spectra were measured to calculate the concentrations of WT-PBS and CB-PBS. The 0.8 M KP buffer was used throughout all of the following reconstitution experiments to maintain the integrity of the PBS and the OCP-PBS complex. The OCP-PBS complexes were prepared by illuminating OCP/PBS mixture for 10 min with intense blue light (482 nm peak, 25.7 nm full width at half maximum (FWHM), 1000 μmol photons m⁻²s⁻¹), with an OCP:PBS molecular ratio of 40:1. The mixture was immediately loaded onto a sucrose gradient with 2.0 M, 1.0 M, 0.5 M and 0.25 M sucrose in 0.8 M KP buffer. The gradient was centrifuged at 50,000 rpm using SW 50.1 centrifuge rotor (Beckman Coulter, Indianapolis, IN, USA) at 23 °C for 3 h. The orange band on the top was discarded and the blue band containing OCP-PBS was carefully collected using a syringe with needle.

2.4. Immunoblot analysis

The PBS and OCP-PBS subunits were partitioned by SDS-PAGE (12% sodium dodecyl sulfate-polyacrylamide gel). All protein samples were desalted before gel electrophoresis by using Amicon ultra centrifugal filters (MilliporeSigma, Burlington, MA, USA). Equal amounts

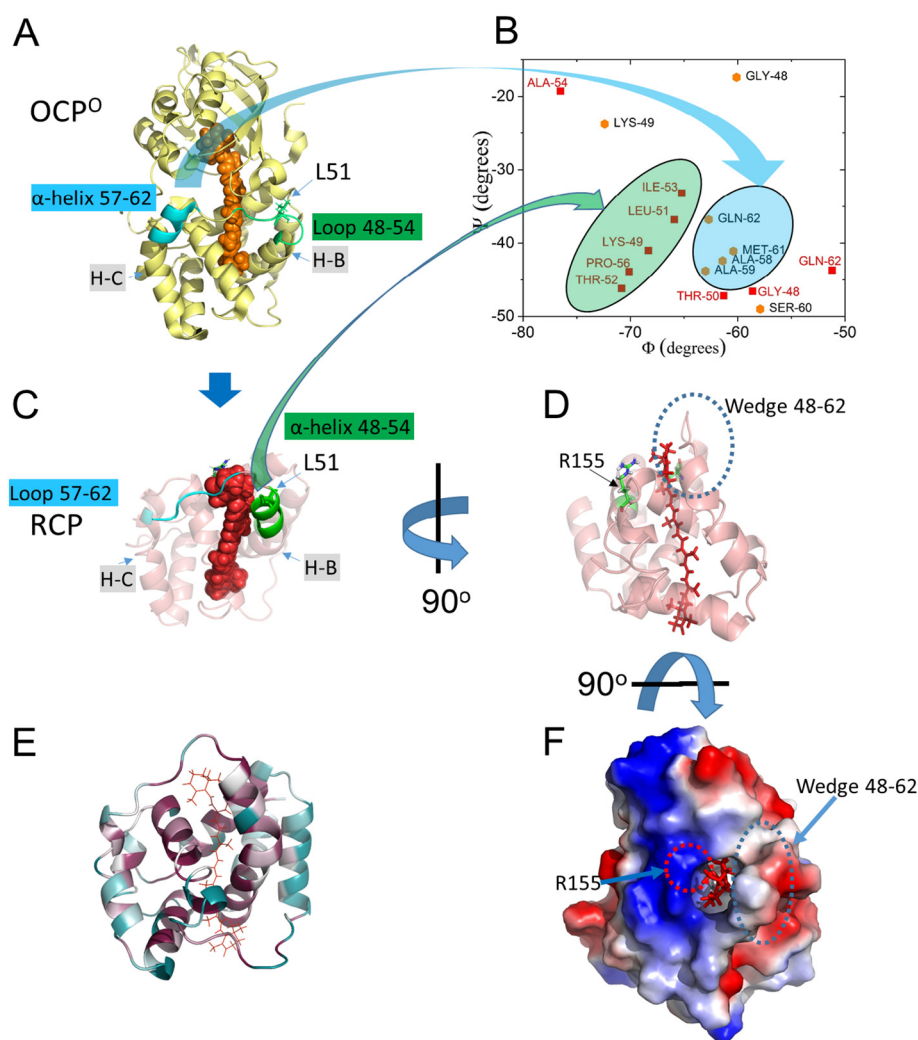


Fig. 1. Secondary structure toggling in OCP^O and RCP. Structural comparison highlighting secondary structure differences in OCP^O (panel A, PDB ID: 4XB5) and RCP (panel C, PDB ID: 4XB4, chain B): peptide 48–54 (green), peptide 57–62 (cyan). (B) Ramachandran analysis showing clustering of ϕ and ψ in α -helix of OCP^O and RCP respectively. (D) Another view of RCP showing a wedge area formed by peptide 48–62, on the opposite side of an essential site for OCP^R binding to PBS. (E) Bioinformatics analysis using the ConSurf server [1,2], showing the conserved domains in OCP that are involved in pigment binding and the loop region of 48–62. Structurally conserved regions are shown as purple, non-conserved regions in teal. (F) Surface electrostatic potential representation of RCP with a rotation of 90° in (D), highlighting surface charges, blue (positively charged), red (negatively), white (non-charged).

of PBS were loaded per lane on SDS-PAGE. Proteins were blotted onto a nitrocellulose membrane and blocked with 5% skim milk for 1 h at room temperature. His-tagged proteins were detected using an anti-polyhistidine monoclonal antibody conjugated with alkaline phosphatase (R932-25, Thermo Fisher Scientific, Waltham, MA, USA) at 1:3000 dilution in 2.5% skim milk at room temperature on a rocking platform and chemiluminescent detection was performed using AP Chemiluminescence technique (SLF1022, Thermo Fisher Scientific, Waltham, MA, USA).

2.5. Steady-state absorption and fluorescence spectroscopy

The absorption spectra of the orange forms of OCPs were collected at room temperature using a UV2510PC Shimadzu UV-VIS spectrophotometer (Shimadzu, Kyoto, Japan). The OCP^R absorption spectrum was recorded at 8 °C (to minimize spontaneous back conversion) after 15 min blue light illumination (482 nm peak, 25.7 nm FWHM, 90 $\mu\text{mol photons m}^{-2}\text{s}^{-1}$) using a Lambda 950 UV-VIS-NIR spectrophotometer (Perkin-Elmer, Waltham, MA, USA). Fluorescence emission spectra of PBS were recorded in a 1-cm path length cuvette with excitation at 580 nm and were monitored using a Cary-Eclipse fluorometer (Varian, Mulgrave, Australia). OCP-mediated fluorescence quenching of excited PBS was induced by 5 min illumination with intense white light (5000 $\mu\text{mol photons m}^{-2}\text{s}^{-1}$). The concentration of PBS was set to 0.013 μM and the molecular ratio of OCP to PBS was 40:1. The concentrations of PBS and OCP were calculated based on sample absorbance values using molar extinction coefficients at those wavelengths:

$$\epsilon_{495 \text{ nm}} = 63,000 \text{ M}^{-1} \text{ cm}^{-1} \text{ for OCP, } \epsilon_{622 \text{ nm}} = 42,660 \text{ mM}^{-1} \text{ cm}^{-1} \text{ for WT-PBS and } \epsilon_{622 \text{ nm}} = 14,220 \text{ mM}^{-1} \text{ cm}^{-1} \text{ for CB-PBS respectively [22,28].}$$

2.6. Time-correlated single photon counting (TCSPC)

Fluorescence decays of phycobilisomes were recorded using a TCSPC setup consisting of a stand-alone Simple-Tau 130 system (Becker & Hickl, Berlin, Germany) equipped with a PMC-100-20 detector with instrument response function of < 200 ps FWHM, PHD-400 – high speed Si pin photodiode as triggering module, motorized Oriel Cornerstone 130 1/8 m monochromator with manually controlled, micrometer adjustable entrance and exit slits, 1200 l/mm grating blazed at 750 nm and manual filter wheel. Excitation pulses matching the PBS absorption maximum (655 nm) were produced by Inspire100, an ultrafast optical parametric oscillator (Spectra-Physics, Santa Clara, CA, USA) pumped with Mai-Tai, an ultrafast Ti:Sapphire laser, generating ~90 fs laser pulses at 820 nm with a frequency of 80 MHz. The frequency of the excitation beam was lowered to 8 MHz by a 3980 Spectra-Physics Pulse Selector. For isotropic excitation of the sample the excitation beam was depolarized using DPU-25 achromatic depolarizer (Thorlab, Newton, NJ, USA). The intensity of the excitation beam was adjusted to ~10¹⁰ photons/cm² per pulse to assure annihilation-free excitation conditions. The excitation beam was focused on the sample in a circular spot of ~1 mm diameter. Fluorescence decay traces were recorded at 680 nm and a 670 nm long pass filter was used at the entrance of the monochromator. Quenching of the PBS

fluorescence emission in PBS/OCP samples was induced by illumination with blue light (482 nm, 25.7 nm FWHM, 1000 $\mu\text{mol photons m}^{-2}\text{s}^{-1}$, 5 min). Fluorescence decay lifetimes were calculated by fitting fluorescence decay traces $F(t)$ with a sum of monoexponential decays according to the general equation:

$$F(t) = \sum_i A_i \exp\left(-\frac{t}{\tau_i}\right) \quad (1)$$

where A_i and τ_i correspond to amplitude and lifetime of each kinetic component. For unquenched PBS samples, fluorescence decay is monoexponential and $i = 1$. However, for quenched PBS multi-exponential decays were necessary to obtain a satisfactory fit. In order to provide a better overall description of these decays that could be used for comparison with unquenched PBS, an amplitude-weighted fluorescence lifetime was calculated according to the equation:

$$\langle \tau \rangle = \frac{\sum_i A_i \tau_i}{\sum_i A_i} \quad (2)$$

3. Results and discussion

3.1. Effect of the L51 mutations on spectroscopic properties of OCP

Rapid heterologous synthesis of large quantities of holo-OCP in *E. coli* [41] helped us choose sites to mutate the loop B amino acids (AAs) L51 and T52 (Fig. 1A). The reasons that these two residues were picked are based on several considerations. (I) These AAs are located in the orifice ring of the pigment cavity, and the dihedral angles φ and ψ values of L51 change from -122.7° , 130.1° in the OCP^O to -65.9° , -36.8° in the OCP^R respectively, and the φ and ψ values of T52 change from -99.7° , 128.2° in the OCP^O to -70.8° , -46.2° in the OCP^R respectively (Fig. 1A, B, C). (II) Consequently, the solvent accessible surface area (SASA) of L51 and T52 undergoes dramatic changes: The SASA value of L51 decreases from 74.5 \AA^2 in the OCP^O (CTD removed, PDBID: 4XB5) to 19.8 \AA^2 (RCP, PDBID: 4XB4, chain B) and those of T52 decreased from 136.6 \AA^2 in the OCP^O to 56.2 \AA^2 in the OCP^R. These changes, together with the previously essential site of R155 (Fig. 1D), which is located on another side of the pigment, indicate the potentially important functional relevance of this site during OCP photoactivation and/or PBS fluorescence quenching.

In this work, all OCPs were expressed and isolated from the *E. coli* system. The absorption spectra of the *E. coli*-expressed OCPs are comparable to the native cyanobacterial OCP (WT-OCP) with only a small red shift (Fig. S1, red line) of absorption peaking at 472 nm and 496 nm with a shoulder at 450 nm, consistent with previous literature reports [41]. Upon blue light illumination, WT- and mutants OCP^O (Fig. 2A, and Fig. S2), except L51T, convert into the red forms, with absorption maximum at 500 nm and a shoulder at 475 nm (Fig. 2B). The L51T-OCP^O mostly precipitated out after elution from the affinity column upon the desalting process (Fig. S2A, inset), indicative of an unstable protein structure.

OCP^O is collectively stabilized by multiple weak molecular forces, such as H-bonds between parts of 3'-hECN and some AAs [13,27]; the connections between the first 19 AAs of NTD with the CTD [44]; and the salt bridge between the NTD and CTD, such as R155 (NTD) and E244 (CTD) [28]. Previous research indicated that changing these AAs reduces the stability of OCP^O, and accelerates OCP^O to OCP^R photoactivation [28]. Absorption spectra of all mutated OCPs were slightly red shifted compared to WT OCP^O. Changing into threonine, a polar amino-acid that potentially increases the solubility of a protein, led to protein precipitation during purification. All this information indicates that in addition to the H-bonds and salt-bridges that affect the OCP stability and photoactivation kinetics, some nonpolar amino-acids could also affect OCP stability, photoactivation, and possibly PBS fluorescence quenching.

3.2. Effect of mutations on the OCP-induced quenching of PBS fluorescence

Quenching capabilities of mutated OCPs were tested on two types of PBS from *Synechocystis* 6803, wild type (WT-PBS), and CB mutant (CB-PBS, a kind gift from Dr. Ajlani [45]) with only one layer of phycocyanin hexamers radially sticking out around it. The room temperature fluorescence emission spectra of the isolated WT-PBS and CB-PBS peak at 665 nm (Fig. 3). As a benchmark for all mutants, WT-OCP was analyzed first. Upon incubation with excess of OCPs in dark (OCP not active), the PBS fluorescence emission spectra show no significant differences. However, when the PBS were illuminated with strong white light for 5 min, fluorescence intensity significantly decreased and blue-shifted, peaking at 661 nm (Fig. 3A, D). In the presence of L51A-OCP, light illumination does not alter the fluorescence emission intensity of both PBSs (WT- and CB-) (Fig. 3B). Additionally, none of the other mutants, L51D, L51K, L51T, showed any PBS fluorescence quenching (Fig. S3). The side chain of T52 is shielded away from solvent in RCP. We thus introduced a point mutation (Alanine) to this site (Fig. S4A). The absorption spectrum of the orange form of T52A-OCP is comparable to that of the WT-OCP and also can be converted to the red, active form upon illumination (Fig. S4B). Upon intense illumination with white light for 5 min, T52A-OCP quenches fluorescence emission of the WT and CB PBS equally well (Fig. S4C and D).

In order to confirm the findings from steady-state fluorescence, picosecond time-resolved fluorescence spectroscopy was applied. This method directly measures PBS fluorescence dynamics and is another way to demonstrate quenching capabilities of OCP. A drop of the PBS fluorescence intensity observed in steady-state spectra should be associated with a decrease of the PBS fluorescence decay lifetime (faster dynamics). The results are given in Fig. 4. The fluorescence decay traces of unquenched PBS were successfully fitted with a monoexponential decay, however OCP-quenched PBS demonstrate fluorescence dynamics with multi-exponential character. In those cases, amplitude weighted lifetimes were calculated (see Materials and methods). The fitting results are provided in Table 1.

The intrinsic fluorescence lifetime of unquenched WT-PBS is 1.89 ns (Fig. 4A), and almost the same value was obtained for CB-PBS, 1.83 ns (Fig. 4D). These time constants are in agreement with previously reported values that range between 1.6 and 1.8 ns [23,25]. When incubated with OCP in the dark (OCP^O), fluorescence decay of both PBS shows no changes in the dynamics (Fig. 4B-F), clearly demonstrating that OCP^O cannot be involved in the quenching mechanism. Upon illumination with intense blue light (482 nm, white light was not used to minimize interference with the detector) for 5 min and in the presence of WT-OCP, the fluorescence decay lifetimes of WT- and CB-PBS shorten to 0.37 ns (Fig. 4B), and to 0.25 ns, respectively. All fluorescence decay lifetimes of PBS obtained for fitting protocols are listed in Table 1.

The observed fluorescence lifetime of PBS is strongly dependent on OCP concentration [23], therefore one would expect that the quenching effect of OCP on both types of PBS will be comparable, however other factors such as accessibility of the binding sites in both PBS may also play a role here.

Importantly, in the presence of the illuminated, red form of L51A-OCP, the fluorescence lifetime of WT- and CB-PBS remained exactly the same as those measured in the presence of its orange form OCP^O (Fig. 4C and F), indicating that spatial arrangement of 3'-hECN in L51A-OCP^R-PBS complex may be substantially different compared to its counterpart from WT-OCP^R-PBS complex. If carotenoid translocation towards specific bilins is essential for effective quenching, then it is possible that mutation of L51 to an alanine completely prevent the carotenoid from moving or making a conformational adjustment in the following stage to a quenching state.

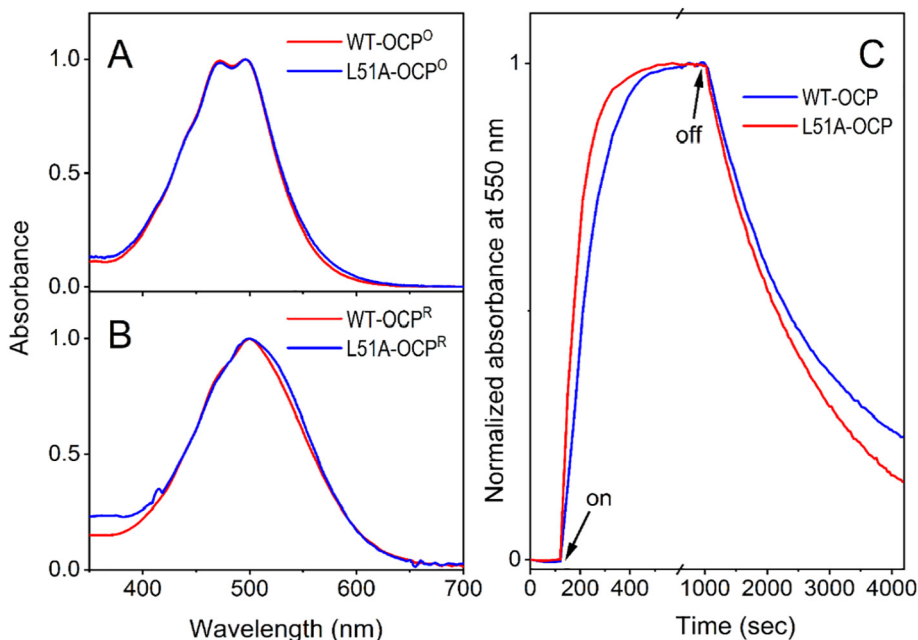


Fig. 2. The absorption spectra of OCPs. The absorption spectrum of (A) OCP^O and (B) OCP^R of WT-OCP and L51A-OCP. (C) The photoactivation kinetics of OCPs were monitored by measuring absorbance changes at 550 nm at 8 °C, under continuous blue light (482 nm, 90 $\mu\text{mol photons m}^{-2}\text{s}^{-1}$). The relaxation kinetics was recorded in darkness at 8 °C. Light “on” or “off” are labeled. Three replicates were performed; representative results are shown here.

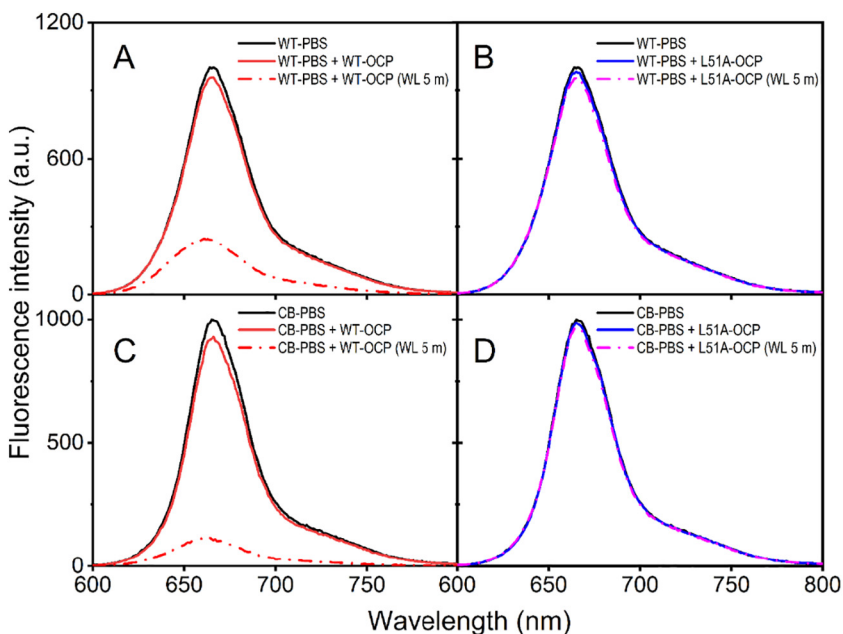


Fig. 3. Room temperature fluorescence emission spectra of the PBS alone or in the presence of OCPs. The fluorescence spectra of WT-PBS (A and B) and CB-PBS (C and D) in the presence of WT-OCP (A and C, red) and L51A-OCP (B and D, blue) after 5 min illumination with white light ($5000 \mu\text{mol photons m}^{-2}\text{s}^{-1}$). The solid lines are the fluorescence emission spectra of WT- and CB-PBS in dark, the dashed spectra are those of WT and CB PBS after illumination. The concentration of WT and CB PBS were 0.013 μM . WL, white light; m, min; a.u., arbitrary units. For fluorescence emission spectra of PBS mixed with other OCP mutants refer to Fig. S3. These are representatives of three replicates.

3.3. Effect of mutations of *Leu51* on ability of OCP to bind to PBS

Both steady state- and time-resolved fluorescence measurements indicated that L51A as well as other OCP mutants (see Fig. S1-3) failed to quench PBS after conversion to OCP^R form induced by light illumination (either white or blue). Previous research reported that decrease or abolishing of PBS fluorescence quenching could be due to altered OCP binding to PBS [6]. Therefore it is a key issue to find if lack of OCP-mediated quenching in the studied samples is due to their inability to form OCP-PBS complexes after OCP activation. To test such possibilities, we performed isolation of OCP-PBS complexes followed by SDS-PAGE and immuno-blot detection (Fig. 5). After the formation of the OCP-PBS complexes during light illumination the OCP-PBS were isolated by centrifugation in a sucrose gradient. The free-floating OCPs were observed in the upper phase of the gradient (the top orange band), and the OCP-PBS complexes were recovered in the 1.0–2.0 M sucrose

fraction (blue band) (Fig. 5A). The presence of OCP bound to PBS was determined by SDS-PAGE followed by immunoblot using monoclonal antibody directed specifically against the polyhistidine tag on OCP. As shown in Fig. 5B and Fig. S5, there is no OCP signal in all dark-adapted OCP-PBS mixtures. After illumination with blue light, WT-OCP was detected in the sample, indicating that prior photoactivation of OCP is required for binding to PBS. However, even after photoactivation, no binding signal of L51D, L51K OCP mutants were observed (Fig. S5). We were not able to collect enough L51T-OCP for binding detection (Fig. S2, inset). Surprisingly, L51A-OCP was observed in a comparable level as WT-OCP after photoactivation. In our previous reports, in the presence of Cu^{2+} , after light illumination, the WT-OCP is locked in its red form and forms a stable PBS-OCP complex [46,47]. It seems, however, that L51A-OCP binds to PBS in a similar stoichiometry to WT-OCP does.

The OCP photo-conversion and OCP^R-induced PBS fluorescence

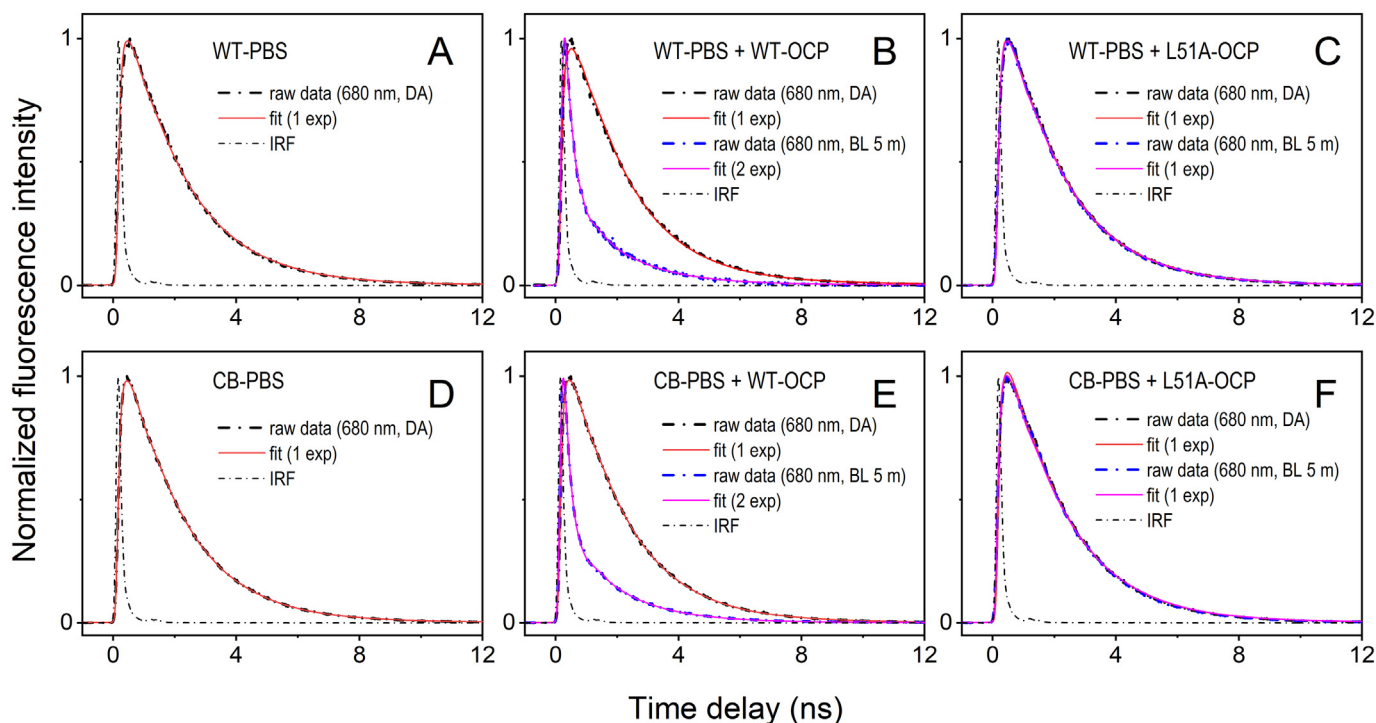


Fig. 4. Time-resolved fluorescence of PBS in dark and incubated with OCP in dark or after illumination with intense blue light (482 nm , $1000\ \mu\text{mol photons m}^{-2}\text{s}^{-1}$, 5 min). The decays were recorded at 680 nm . The molecular ratio of OCP to PBS was $40:1$. All traces are normalized to unity for better temporal comparison. DA, dark-adapted; BL, blue light; m, minute; IRF – instrument response function. The experiments were repeated three times.

Table 1

Fluorescence decay lifetimes of the WT- and CB-PBS in the presence of WT- and L51A-OCP in dark or after 5 min illumination with intense blue light (482 nm , $1000\ \mu\text{mol photons m}^{-2}\text{s}^{-1}$). The molecular ratio of OCP to PBS is $40:1$.

Samples	Lifetime [amplitude] (ns)		a-w lifetime (ns)
PBS	1.89		
PBS + WT-OCP (dark)	1.82		
PBS + WT-OCP (BL 5 min)	1.72 [0.16]	0.17 [0.84]	0.37
PBS + L51A-OCP (dark)	1.89		
PBS + L51A-OCP (BL 5 min)	1.89		
CB	1.83		
CB + WT-OCP (dark)	1.86		
CB + WT-OCP (BL 5 min)	1.7 [0.01]	0.14 [0.99]	0.25
CB + L51A-OCP (dark)	1.90		
CB + L51A-OCP (BL 5 min)	1.90		

BL, blue light, a-w – amplitude-weighted.

quenching are two discrete events in the OCP-related NPQ mechanism. Photoactivation of OCP^{O} to OCP^{R} is required for photoprotection but is not sufficient [28]. The absorption spectra and the stability of the red form of the mutant OCPs were the same as that of the WT-OCP, which means that mutant OCPs can accumulate the red, active form OCP^{R} as well as WT-OCP does (Fig. 1B and C, Fig. S2B). However, all L51A, L51D, L51K, and L51T OCP mutants were unable to induce the PBS fluorescence quenching (Figs. 3, 4, and Fig. S3). Binding experiments indicated that the absence of PBS fluorescence quenching of L51D- and L51K-OCP are due to a failure to bind to the PBS. However, L51A-OCP binds to PBS in a similar level as WT-OCP. This result demonstrates that formation of an OCP^{R} -PBS binding complex is not the same as formation of an OCP^{R} -PBS “quenching” complex. The introduction of an Alanine in the L51 site in OCP completely abolished the formation of a quenching state of the OCP^{R} -PBS complex. It is unlikely that L51A-OCP^R binds to PBS at a different site. However, probing the accurate binding domain of OCP on PBS remains a technical challenge at

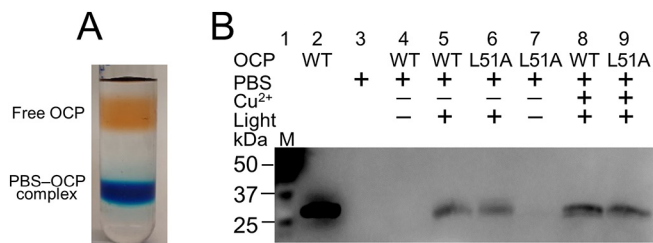


Fig. 5. Detection of OCP in the isolated OCP-PBS complex formed after OCP activation in the PBS/OCP mixture. (A) Sucrose gradient ultracentrifugation of OCP-PBS complex (representative). (B) Immuno-detection of OCP in OCP-PBS complex, wild type (WT) or mutant (L51A) OCP protein, in the absence/presence of blue light illumination ($1000\ \mu\text{mol photons m}^{-2}\text{s}^{-1}$ for 10 min) and absence/presence of Cu^{2+} . First lane contains protein marker (M), the molecular weight of which are labeled as kDa. Note: both WT and OCP mutant are C-terminally His₆-tagged. Monoclonal anti-polyhistidine antibody was used. Each well contains $15\ \mu\text{l}$ of $1\ \mu\text{M}$ PBS.

the present time. Negatively charged or positively charged AAs in place of leucine, L51D and L51K, however, entirely blocked binding of the OCP to PBS, resulting in no fluorescence quenching (Fig. S3). Our results suggest that lack of binding capabilities of L51D-OCP and L51K-OCP to PBS is probably caused by losing a large non-polar residue that collectively contributes to the hydrophobic interaction between OCP^{R} and the PBS core. Bioinformatics analysis based on 100 full-length OCP sequences compiled from the genome of the strains (Fig. 1E) indeed showed that this site is highly conservatively occupied by either Isoleucine (I), Leucine (L), or Valine (V), so called branched-chain AAs and the most hydrophobic AAs and play crucial roles in determining the structures of the globular proteins.

It remains unknown if any possible post-binding events occur during the OCP photoprotection cycle. It was assumed that the secondary structures of NTD and CTD of OCP^{R} have no large conformational differences [20,27]. This view was mostly derived from the

crystalized RCP, supposedly the equivalent of NTD of OCP^R, with a root mean square deviation of 1.24 Å compared with NTD of OCP^O [20]. However, the 12 Å translocation of the carotenoid concomitant with the complete separation of NTD and CTD raises the possibility of an additional/reverse carotenoid structural movement after binding of OCP^R to PBS, suggesting that the carotenoid molecule could closely approach to the bilin molecule(s) where the excitation energy has to be quenched. Alternatively, the mutation hinders the proper orientation of the OCP in the PBS core that prevents the action of quenching process. It has been shown that OCP residue R155 is essential for formation of the OCP^R-PBS quenching complex [28] and it is located on one side of the orifice that holds the carotenoid head group (Fig. 1C, D). We hypothesize that other sites around the carotenoid molecule opening could also play important roles, regulating pigment back and forth movement. By comparing the available protein structures of OCP^O (PDBID: 4XB5) and RCP (PDBID: 4XB4) [20], we noticed that there are significant conformational differences in a peptide fragment (Loop B) containing 14 AAs (48–62 AA) that connect helix B and helix C: Peptide 48–54 is a free loop in OCP^O vs an α -helix in OCP^R as an extension of helix B with a bent towards the pigment (Fig. 1A, C). In contrast, peptide 57–62 is a fraction of α -helix C in OCP^O vs a loop in OCP^R. Indeed, there is no significant secondary structure percentage change, since the α -helix extension of helix B is cancelled out by shortening of α -helix C into a loop (peptide 57–62). L51 is located in such loop region in OCP^O and it participates in formation of α -helix in OCP^R.

4. Conclusions

Using a heterologous expression system, we successfully identified an essential site in OCP that is involved in PBS binding and photoprotection. Previous research demonstrated that charged AAs are required for the OCP binding to PBS [28]. Our results indeed expand this concept and demonstrate that a site occupied by a hydrophobic AA in a conserved loop region of OCP^O plays an essential role for forming a proper OCP^R-PBS quenching complex. Additionally, our results (L51A) support the hypothesis that simple binding of OCP^R to PBS is not sufficient for its functional role as an excitation energy quencher, strongly indicating that a further structural rearrangement may be required to trigger the quenching process, so that OCP may adopt an as-yet-unknown structure, considering that L51 is located in a region that adopts significantly different secondary structures of two OCP states. Protein footprinting using structural mass spectrometry proteomics methods are underway to probe the changes in WT-OCP-PBS and L51A-OCP-PBS, although there are technical challenges in stabilizing them when subjected to footprinting chemistry.

Declaration of competing interest

There is no research interest conflict associated with this research.

Acknowledgements

This research is funded by the U.S. Department of Energy (DOE), Office of Basic Energy Sciences (Grant DE-FG02-07ER15902 to R.E.B and H.L.) W. L. was funded by the DOE grant. Time-resolved spectroscopic studies were performed in the ultrafast laser facility funded by U.S. Department of Energy (DOE), Office of Basic Energy Sciences (Grant DE-SC0001035 to R.E.B). D. M. N. acknowledges the Center for Solar Energy and Energy Storage and the McKelvey School of Engineering at Washington University in St Louis for financial support. The authors would like to thank Blankenship laboratory members for collegial discussions and technical support.

Appendix A. Supplementary data

Supplementary data to this article can be found online at <https://>

doi.org/10.1016/j.bbabi.2020.148155.

References

- [1] O. Goldenberg, et al., The ConSurf-DB: pre-calculated evolutionary conservation profiles of protein structures, *Nucleic Acids Res.* 37 (Database issue) (2009) D323–D327.
- [2] M. Landau, et al., ConSurf 2005: the projection of evolutionary conservation scores of residues on protein structures, *Nucleic Acids Res.* 33 (Web Server issue) (2005) W299–W302.
- [3] K. El Bissati, et al., Photosystem II fluorescence quenching in the cyanobacterium *Synechocystis* PCC 6803: involvement of two different mechanisms, *Biochim. Biophys. Acta* 1457 (3) (2000) 229–242.
- [4] A. Wilson, et al., A soluble carotenoid protein involved in phycobilisome-related energy dissipation in cyanobacteria, *Plant Cell* 18 (4) (2006) 992–1007.
- [5] A.V. Ruban, et al., Identification of a mechanism of photoprotective energy dissipation in higher plants, *Nature* 450 (7169) (2007) 575–578.
- [6] D. Kirilovsky, C.A. Kerfeld, Cyanobacterial photoprotection by the orange carotenoid protein, *Nature Plants* 2 (12) (2016).
- [7] K.K. Niyogi, T.B. Truong, Evolution of flexible non-photochemical quenching mechanisms that regulate light harvesting in oxygenic photosynthesis, *Curr. Opin. Plant Biol.* 16 (3) (2013) 307–314.
- [8] H. Liu, H. Zhang, D.M. Niedzwiedzki, M. Prado, G. He, M.L. Gross, R.E. Blankenship, Phycobilisomes supply excitations to both photosystems in a megacalkenox in cyanobacteria, *Science* 342 (6162) (2013) 1104–1107.
- [9] C.W. Mullineaux, Phycobilisome-reaction centre interaction in cyanobacteria, *Photosynth. Res.* 95 (2–3) (2008) 175–182.
- [10] M. Yokono, A. Murakami, S. Akimoto, Excitation energy transfer between photosystem II and photosystem I in red algae: larger amounts of phycobilisome enhance spillover, *Biochim. Biophys. Acta* 1807 (7) (2011) 847–853.
- [11] D. Kirilovsky, C.A. Kerfeld, The Orange Carotenoid Protein: a blue-green light photoactive protein, *Photochem Photobiol Sci* 12 (7) (2013) 1135–1143.
- [12] T.K. Holt, D.W. Krogmann, A carotenoid-protein from cyanobacteria, *Biochim. Biophys. Acta* 637 (3) (1981) 408–414.
- [13] C.A. Kerfeld, et al., The crystal structure of a cyanobacterial water-soluble carotenoid binding protein, *Structure* 11 (1) (2003) 55–65.
- [14] D. Kirilovsky, Photoprotection in cyanobacteria: the orange carotenoid protein (OCP)-related non-photochemical-quenching mechanism, *Photosynth. Res.* 93 (1–3) (2007) 7–16.
- [15] T. Polivka, et al., Spectroscopic properties of the carotenoid 3'-hydroxyechinenone in the orange carotenoid protein from the cyanobacterium *Arthrospira maxima*, *Biochemistry* 44 (10) (2005) 3994–4003.
- [16] D.M. Niedzwiedzki, H. Liu, R.E. Blankenship, Excited state properties of 3'-hydroxyechinenone in solvents and in the Orange Carotenoid Protein from *Synechocystis* sp. PCC 6803, *J. Phys. Chem. B* 118 (23) (2014) 6141–6149.
- [17] A. Wilson, et al., A photoactive carotenoid protein acting as light intensity sensor, *Proc. Natl. Acad. Sci. U. S. A.* 105 (33) (2008) 12075–12080.
- [18] D. Jallet, et al., Specificity of the cyanobacterial orange carotenoid protein: influences of orange carotenoid protein and phycobilisome structures, *Plant Physiol.* 164 (2) (2014) 790–804.
- [19] H. Liu, et al., Mass spectrometry footprinting reveals the structural rearrangements of cyanobacterial orange carotenoid protein upon light activation, *Biochim. Biophys. Acta* 1837 (12) (2014) 1955–1963.
- [20] R.L. Leverenz, et al., PHOTOSYNTHESIS. A 12 A carotenoid translocation in a photoswitch associated with cyanobacterial photoprotection, *Science* 348 (6242) (2015) 1463–1466.
- [21] R. Berera, et al., The photophysics of the orange carotenoid protein, a light-powered molecular switch, *J. Phys. Chem. B* 116 (8) (2012) 2568–2574.
- [22] M. Gwizdzala, A. Wilson, D. Kirilovsky, In vitro reconstitution of the cyanobacterial photoprotective mechanism mediated by the Orange Carotenoid Protein in *Synechocystis* PCC 6803, *Plant Cell* 23 (7) (2011) 2631–2643.
- [23] I.N. Stadnichuk, et al., Site of non-photochemical quenching of the phycobilisome by orange carotenoid protein in the cyanobacterium *Synechocystis* sp. PCC 6803, *Biochim. Biophys. Acta* 1817 (8) (2012) 1436–1445.
- [24] A.H. Squires, et al., Single-molecule trapping and spectroscopy reveals photophysical heterogeneity of phycobilisomes quenched by Orange Carotenoid Protein, *Nat. Commun.* 10 (1) (2019) 1172.
- [25] L. Tian, et al., Picosecond kinetics of light harvesting and photoprotective quenching in wild-type and mutant phycobilisomes isolated from the cyanobacterium *Synechocystis* PCC 6803, *Biophys. J.* 102 (7) (2012) 1692–1700.
- [26] L.J. Tian, et al., Site, rate, and mechanism of photoprotective quenching in cyanobacteria, *J. Am. Chem. Soc.* 133 (45) (2011) 18304–18311.
- [27] R.L. Leverenz, et al., Structural and functional modularity of the orange carotenoid protein: distinct roles for the N- and C-terminal domains in cyanobacterial photoprotection, *Plant Cell* 26 (1) (2014) 426–437.
- [28] A. Wilson, et al., The essential role of the N-terminal domain of the orange carotenoid protein in cyanobacterial photoprotection: importance of a positive charge for phycobilisome binding, *Plant Cell* 24 (5) (2012) 1972–1983.
- [29] Y. Lu, et al., A molecular mechanism for nonphotochemical quenching in cyanobacteria, *Biochemistry* 56 (22) (2017) 2812–2823.
- [30] H. Zhang, et al., Molecular mechanism of photoactivation and structural location of the cyanobacterial orange carotenoid protein, *Biochemistry* 53 (1) (2014) 13–19.
- [31] D. Harris, et al., Orange carotenoid protein burrows into the phycobilisome to provide photoprotection, *Proc. Natl. Acad. Sci. U. S. A.* 113 (12) (2016) E1655–E1662.

- [32] F.I. Kuzminov, et al., Investigation of OCP-triggered dissipation of excitation energy in PSI/PSII-less *Synechocystis* sp. PCC 6803 mutant using non-linear laser fluorimetry, *Biochim. Biophys. Acta* 1817 (7) (2012) 1012–1021.
- [33] R.R. Sonani, et al., Site, trigger, quenching mechanism and recovery of non-photochemical quenching in cyanobacteria: recent updates (vol 137, pg 171, 2018), *Photosynth. Res.* 137 (2) (2018) 181–182.
- [34] I.N. Stadnichuk, et al., Fluorescence quenching of the phycobilisome terminal emitter L from the cyanobacterium *Synechocystis* sp. PCC 6803 detected in vivo and in vitro, *J. Photochem. Photobiol. B* 125C (2013) 137–145.
- [35] D.V. Zlenko, P.M. Krasilnikov, I.N. Stadnichuk, Role of inter-domain cavity in the attachment of the orange carotenoid protein to the phycobilisome core and to the fluorescence recovery protein, *J. Biomol. Struct. Dyn.* 34 (3) (2016) 486–496.
- [36] E.G. Maksimov, et al., Hybrid coupling of R-phycoerythrin and the orange carotenoid protein supports the FRET-based mechanism of cyanobacterial photoprotection, *Biochem. Biophys. Res. Commun.* 516 (3) (2019) 699–704.
- [37] E.G. Maksimov, et al., The photocycle of orange carotenoid protein conceals distinct intermediates and asynchronous changes in the carotenoid and protein components, *Sci. Rep.* 7 (1) (2017) 15548.
- [38] P.E. Konold, et al., Photoactivation mechanism, timing of protein secondary structure dynamics and carotenoid translocation in the Orange Carotenoid Protein, *J. Am. Chem. Soc.* 141 (1) (2019) 520–530.
- [39] E.G. Maksimov, et al., The signaling state of Orange carotenoid protein, *Biophys. J.* 109 (3) (2015) 595–607.
- [40] T. Polivka, P. Chabera, C.A. Kerfeld, Carotenoid-protein interaction alters the S(1) energy of hydroxyechinenone in the Orange Carotenoid Protein, *Biochim. Biophys. Acta* 1827 (3) (2013) 248–254.
- [41] C.B. de Carbon, et al., Biosynthesis of soluble carotenoid holoproteins in *Escherichia coli*, *Sci. Rep.* 5 (2015).
- [42] A.N. Glazer, Phycobiliproteins, *Methods Enzymol.* 167 (1988) 291–303.
- [43] B. Ughy, G. Ajlani, Phycobilisome rod mutants in *Synechocystis* sp. strain PCC6803, *Microbiology* 150 (Pt 12) (2004) 4147–4156.
- [44] A. Thurotte, et al., Regulation of Orange Carotenoid Protein activity in cyanobacterial photoprotection, *Plant Physiol.* 169 (1) (2015) 737–747.
- [45] G. Ajlani, C. Verotte, Construction and characterization of a phycobiliprotein-less mutant of *Synechocystis* sp. PCC 6803, *Plant Mol. Biol.* 37 (3) (1998) 577–580.
- [46] H. Liu, et al., Photoactivation and relaxation studies on the cyanobacterial orange carotenoid protein in the presence of copper ion, *Photosynth. Res.* 135 (1–3) (2018) 143–147.
- [47] W. Lou, et al., Cu(+) contributes to the orange carotenoid protein-related phycobilisome fluorescence quenching and photoprotection in cyanobacteria, *Biochemistry* 58 (28) (2019) 3109–3115.